

# The origin of power-law distributions in deterministic walks: the influence of landscape geometry

M. C. Santos,<sup>1</sup> D. Boyer,<sup>2</sup> O. Miramontes,<sup>2</sup> G. M. Viswanathan,<sup>3</sup> E. P. Raposo,<sup>4</sup> J. L. Mateos,<sup>2</sup> and M. G. E. da Luz<sup>1,\*</sup>

<sup>1</sup>Departamento de Física, Universidade Federal do Paraná, 81531-990 Curitiba-PR, Brazil.

<sup>2</sup>Departamento de Sistemas Complejos, Instituto de Física, Universidad Nacional Autónoma de México, Apartado Postal 20-364, 01000 México D.F., México

<sup>3</sup>Instituto de Física, Universidade Federal de Alagoas, 57072-970 Maceió-AL, Brazil

<sup>4</sup>Laboratório de Física Teórica e Computacional, Departamento de Física, Universidade Federal de Pernambuco, 50670-901 Recife-PE, Brazil

We investigate the properties of a deterministic walk, whose locomotion rule is always to travel to the nearest site. Initially the sites are randomly distributed in a closed rectangular ( $A/L \times L$ ) landscape and, once reached, they become unavailable for future visits. As expected, the walker step lengths present characteristic scales in one ( $L \rightarrow 0$ ) and two ( $A/L \sim L$ ) dimensions. However, we find scale invariance for an intermediate geometry, when the landscape is a thin strip-like region. This result is induced geometrically by a dynamical trapping mechanism, leading to a power law distribution for the step lengths. The relevance of our findings in broader contexts – of both deterministic and random walks – is also briefly discussed.

PACS numbers: 89.75.Fb, 89.75.Da, 05.40.Fb, 05.50.+q, 05.40.-a

## I. INTRODUCTION

A large number of phenomena in physics, ecology, chemistry, economics, etc [1, 2, 3], characterized by scale invariant distributions, are in many situations associated with Lévy walks and Lévy flights [4, 5, 6]. Furthermore, when related to diffusion mechanisms, these types of systems present mean square displacements that, for large enough times [7], scale as  $t^\alpha$  with  $\alpha > 1$ .

In such contexts, some of the relevant challenges are to determine: (a) if there are global driving forces underlying the superdiffusive features; (b) how they can emerge; and (c) how they are linked to other properties such as self-similarity, fractality, noise with  $f^{-\beta}$  power spectrum and intermittent bursts behavior, ubiquitous in Nature [8]. In fact, many studies address such general questions under different perspectives. For instance, one idea points to the concept of self-organized criticality [9]. The so called spatiotemporal complex systems evolve through a series of avalanches towards critical states, which possess scale invariance and long range correlations. These hierarchical “paths” are unavoidable due to the character of the dynamics and are observed in many problems [10]. For deterministic chaotic systems, on the other hand, the above queries may be associated either to dynamical fractional kinetics [2] or to phase space strange non-chaotic attractors and attracting sets of particular geometrical partitions (see [11] and refs. therein).

In the realm of stochastic processes, especially random walks, there are different direct causes for superdiffusion and power-law tailed decay. To exemplify just a few of them, we mention: (i) the evolution governed by fractional Fokker-Planck equations [1]; (ii) dichotomic sys-

tems for which two time scales, microscopic and macroscopic [12], can be identified; (iii) the existence of correlations in the variance of the physically relevant quantities [13]; and (iv) random multiplicative processes in the presence of a boundary constraint (a repelling barrier) [14]. Moreover, it may happen that a Lévy or power law distribution for the dynamical variables of a random process may be a natural way to lead to certain outcomes such as: the diversity of species in evolutionary ecology [15]; efficiency optimization in random search, e.g., animal foraging [16] in continuous Euclidean spaces [17, 18, 19, 20, 21, 22, 23] and targets search in discrete lattice environments [24]; and to avoid the extinction edge in scenarios of low availability of energetic resources [25].

There is a much less studied class of problems known as deterministic walks [26, 27, 28]. As in the usual stochastic case, they describe the movement of a walker in a certain medium, which can or cannot have a random character. However, the rule of locomotion is always taken from some purely deterministic model, rather than from a probability distribution [28]. Deterministic walks usually present the technical difficulties common to nonlinear dynamical systems [26] and can give rise to superdiffusive processes [28]. In fact, they belong to a new class of models known as local optimization problems, such as the traveling tourist [26]. In contrast to the previously discussed examples of purely random walks, it seems that for deterministic walks there are no general guidelines indicating when the evolution would generate power-law distributions for the dynamical variables.

In the present contribution we study the previous general questions for a specific deterministic walk. We revisit a recently proposed model [29], in which the walker moves in straight lines from site to site, following a “go to the closest target site” rule. The sites are randomly distributed in a 2D region. As already pointed out in [29],

\*Electronic address: luz@fisica.ufpr.br

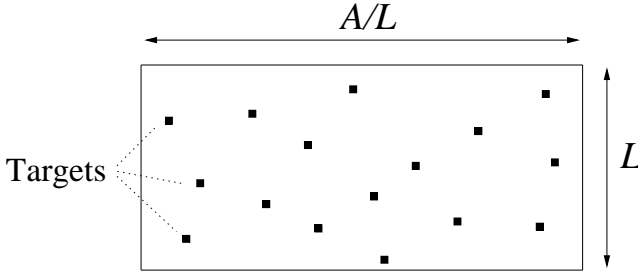


FIG. 1: Schematics of the search space where the small squares represent the randomly distributed target sites.

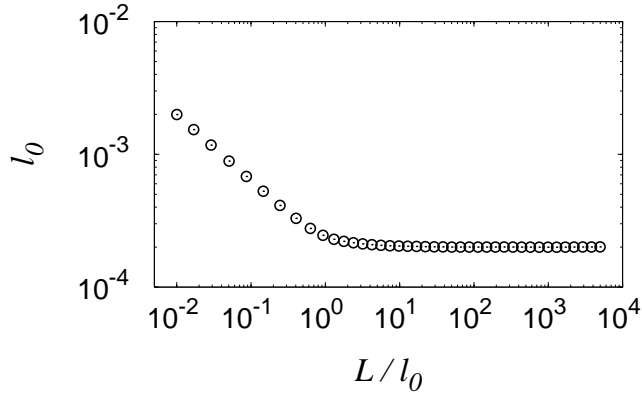


FIG. 2:  $\ell_0$  as function of  $L/\ell_0$ . For  $L/\ell_0 \gg 1$  (2D regime),  $\ell_0$  is the constant  $1/\sqrt{N}$ , whereas for  $L/\ell_0 \ll 1$  (1D),  $\ell_0$  goes as  $1/(NL)$ . The crossover takes place for  $L/\ell_0$  around unity.

for certain very particular parameter conditions, this type of dynamics surprisingly exhibits power law distribution of step lengths. Here we reveal the mechanisms leading to such behavior, not analyzed in [29], showing that the crossover is due to a trapping effect associated to particular spatial configurations of the landscape. The onset of this phenomenon resembles a critical point in thermodynamics, even though there is no real phase transition in the system.

The paper is organized as follows. In Sec. II we propose the model. Simulations are presented in Sec. III. In Sec. IV we discuss and interpret our findings. Final remarks and conclusion are drawn in Sec. V.

## II. THE MODEL

We consider a deterministic walk model that was originally presented in Ref. [29] to describe the locomotion of spider monkeys during foraging [20]. We define a rectangular region of area  $A$  and length  $L_1 = L$  and  $L_2 = A/L$  along the vertical ( $y$ -axis) and horizontal ( $x$ -axis) directions, respectively. Within this domain, a total

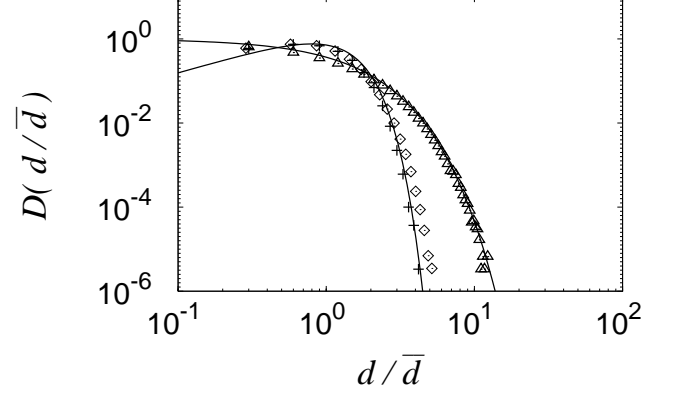


FIG. 3: The numerically calculated distributions of distances between closest neighbor sites for three values of  $L/\ell_0$  (see main text), corresponding to the: 2D (cross), 1D (triangle) and crossover region (diamond) cases. The respective analytical distributions fitting 2D and 1D are plotted as solid lines. Note that the intermediate (crossover) is close to the 2D case.

of  $N$  point targets are initially distributed at random. The configuration of the search region is schematically represented in Fig. 1. In all the simulations we set  $N = 2.5 \times 10^7$  and  $A = 1$ . The dynamics is given by the two following simple rules:

- Once at a certain target site, the walker moves straight to the closest available site.
- The walker does not come back to any previously visited site – the search is destructive, i.e., the total number of sites decreases as they are found along the walk.

Let us define the characteristic length

$$\ell_0 = 2\bar{d} \quad (1)$$

with

$$\bar{d} = \frac{1}{N} \sum_n d_n, \quad (2)$$

where  $d_n$  is the distance between the target  $n$  and its closest neighbor. As  $L$  can be taken in the interval  $[0, 1]$ , we have two limiting cases. When  $L = \mathcal{O}(1)$ , the process takes place in a 2D space and  $\ell_0 = \sqrt{1/N}$ . On the other hand, as  $L \rightarrow 0$  the domain is 1D and  $\ell_0 = 1/(LN)$ . The crossover between these two regimes is found by varying  $L$ . Fig. 2 displays the numerically calculated  $\ell_0$  as a function of  $L/\ell_0$ . The two limiting behaviors are clearly seen and separated by a crossover emerging around  $L/\ell_0 \approx 1$ . In the following, we will use  $L/\ell_0$  as the main parameter of the model.

In Fig. 3 we display the distribution  $D(d/\bar{d})$  of the separation distances  $d_n$  for the three situations: the 2D limit with  $L/\ell_0 \approx 4978.56$  ( $L = 1$  and  $\ell_0 = 2.00861 \times 10^{-4}$ ), the 1D-limit with  $L/\ell_0 \approx 9.99474 \times 10^{-3}$  ( $L = 2 \times 10^{-5}$

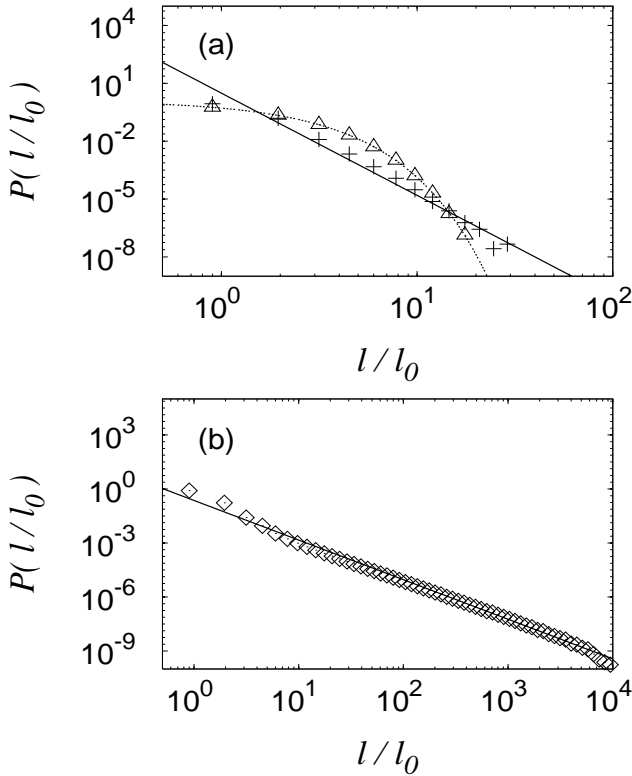


FIG. 4: Normalized step length distributions for the same parameters as in Fig. 3. (a) The triangles (cross) represents the 1D (2D) limit. The curves show the fits  $1.3 \exp[-0.92 \ell/\ell_0]$  (dashed) and  $3.1 (\ell/\ell_0)^{-5.3}$  (continuous). (b) The intermediate case (diamond). Here the fit is  $0.23 (\ell/\ell_0)^{-2.2}$ .

and  $\ell_0 = 2.00105 \times 10^{-3}$ ), and in the crossover region with  $L/\ell_0 \approx 4.21598$  ( $L = 8.82 \times 10^{-4}$  and  $\ell_0 = 2.09204 \times 10^{-4}$ ). The expected distributions, Poisson  $D(d/\bar{d}) = \exp[-d/\bar{d}]$  and the standard Weibull (i.e., a weighted Gaussian)  $D(d/\bar{d}) = (\pi/2) d/\bar{d} \exp[-\pi d^2/(4\bar{d}^2)]$ , respectively in the 1D and 2D cases, are recovered.

### III. RESULTS

We simulate the walks by iterating our two rules for various values of  $L/\ell_0$ . Each simulation runs until the walker visits  $10^5$  targets, out of the initial  $N = 2.5 \times 10^7$ . The curves are obtained by averaging over  $10^3$  runs. At  $t = 0$ , the walker is located on a site in the vicinity of the center of the searching environment.

A first important quantity is the distribution  $P(\ell/\ell_0)$  of the reduced distance  $\ell/\ell_0$  traveled by the walker between two consecutive target sites. In Fig. 4(a) we show the results corresponding to the 1D and 2D cases of Fig. 3. For 1D, the curve follows the expected exponential Poisson distribution. For 2D,  $P(\ell/\ell_0)$  differs markedly from the standard Weibull (i.e., a weighted Gaussian) distribution of nearest distances  $D(d/\bar{d})$ . The

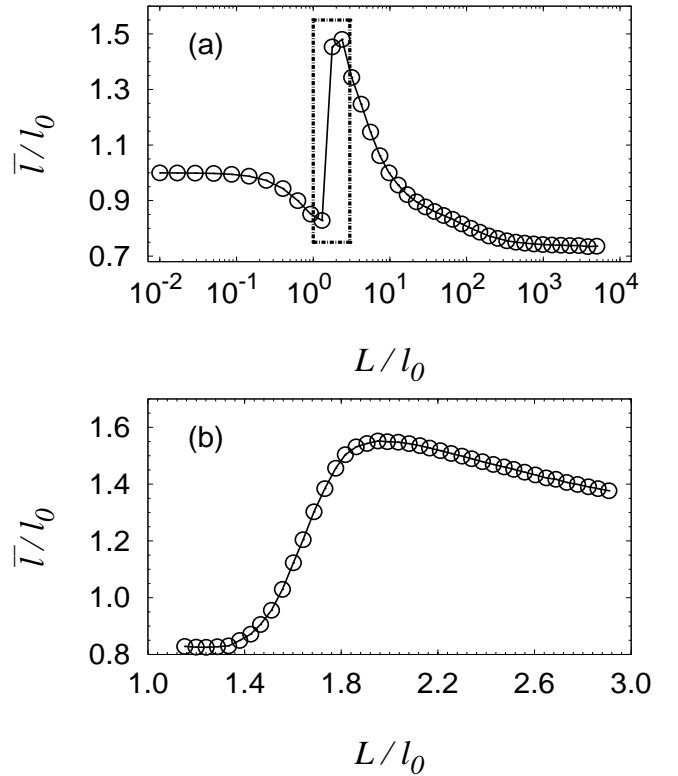


FIG. 5: (a) The numerical average step length  $\bar{\ell}$  (in units of  $\ell_0$ ) taken by the walker during the search as function of  $L/\ell_0$ . The region where  $\bar{\ell}$  presents a peak, indicated by a rectangle, is shown in detail in (b). The continuous curves are just guides for the eye.

curve is broader, but can be well fitted by a rapidly decaying inverse power-law with exponent close to 5.3, whose general behavior is actually Gaussian, driven by the Central Limit Theorem with converging second moment [4]. However, for the example in the crossover region,  $L/\ell_0 \approx 4.21598$ ,  $P$  clearly exhibits a very long tail, as shown in Fig. 4 (b). There is a small but non-negligible probability of long walks. In this case, we find numerically that  $P \sim (\ell/\ell_0)^{-\mu}$  with  $\mu \approx 2.2$  ( $\mu \approx 2.15$  by considering only the interval  $10 < \ell/\ell_0 < 10^4$ ). Thus, the distribution has a power-law behavior with a diverging second moment, similar to Lévy processes.

A second relevant quantity is the reduced average step length  $\bar{\ell}/\ell_0$ , displayed in Fig. 5 (a) as a function of  $L/\ell_0$ . As shown in more detail in Fig. 5 (b), we have a peak for  $\bar{\ell}/\ell_0$  in the crossover region, with the maximum corresponding to  $L/\ell_0 \approx 1.99 \approx 2$ .

From the Fig. 5 we are lead to think that the step lengths in the crossover region are indeed larger than those for the 1D and 2D limits. In fact, we find this is true within the interval  $2 < L/\ell_0 < 30$ , where the distribution  $P(\ell/\ell_0)$  can fairly be written as  $(\ell/\ell_0)^{-\mu}$  with  $2 < \mu < 3$ . For some values of  $L/\ell_0$ , we list in Table I the corresponding power-law exponents  $\mu$ . Some step lengths

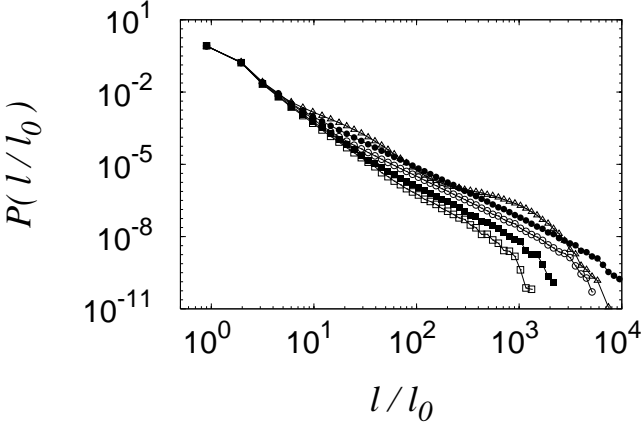


FIG. 6: The distribution  $P(l/l_0)$  fitted as  $(l/l_0)^{-\mu}$ . The parameters are:  $L/l_0 = 2.37957$  and  $\mu = 2.3155$  (open triangle);  $L/l_0 = 4.21598$  and  $\mu = 2.22267$  (full circle);  $L/l_0 = 9.74390$  and  $\mu = 2.40229$  (open circle);  $L/l_0 = 22.1615$  and  $\mu = 2.65706$  (full square); and  $L/l_0 = 38.2288$  and  $\mu = 2.96385$  (open square).

TABLE I: For some values of  $2 < L/l_0 < 30$ , the fitted  $\mu$ 's for  $P(l/l_0)$  written as  $(l/l_0)^{-\mu}$ .

$L/l_0$	$\mu$
2.37957	2.31550
3.17214	2.28575
4.21598	2.22267
5.58647	2.28323
7.38735	2.33486
9.74390	2.40229
12.8287	2.48336
16.8655	2.52824
22.1615	2.65706
29.1083	2.78089

distributions are shown in Fig. 6. For comparison we also plot the example of Fig. 4 (b).

#### IV. DISCUSSION

To understand the above results we turn to the dynamics of the deterministic search process. In the 1D limit ( $L \rightarrow 0$ ) the random walker tends to follow an almost straight line, with only a few changes in direction, mostly occurring during the first steps. On the other hand, the 2D limit ( $L \rightarrow 1$ ) is characterized by a much larger available space in both directions. Although the destruction of previously visited sites makes the walker tend to move forwards with higher probability, there is a finite fraction of large turning angles along the walk. To quantify these features we present in Fig. 7 a normalized plot of the angular distribution  $\Gamma(\theta)$  of angles between two consecutive steps corresponding to the examples of

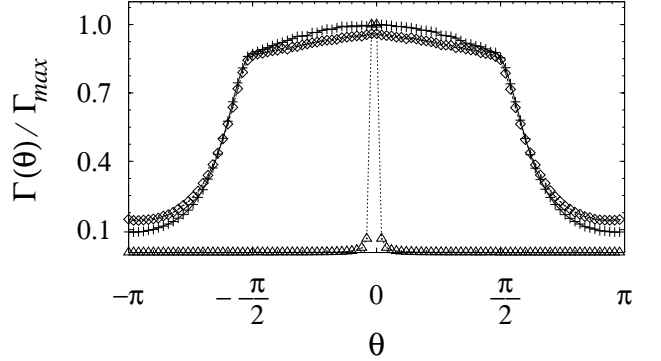


FIG. 7: Angular distribution of the turning angles between consecutive steps. The triangles (1D), crosses (2D) and diamonds (crossover region) correspond to the same cases of Fig. 4. The dotted curve (for the triangles) is just a guide for the eye.

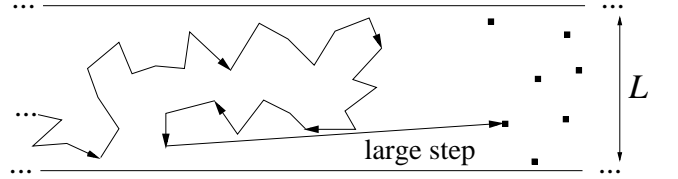


FIG. 8: In the crossover regime, the search space is a narrow strip. In such case, a walker moving in average to the right may perform many steps in the opposite direction, returning near the rightmost visited site through a very long step.

Fig. 4. In the 1D limit, the distribution is very peaked at small angle values, indicating that the walker rarely deviates from a certain direction (either left or right, defined shortly after a few initial steps). In the 2D limit there is a bias toward the forward direction, nevertheless larger angles are also likely to happen.

It is, however, interesting to notice that Fig. 7 alone is not sufficient to explain our findings, since the 2D and crossover cases present similar  $\Gamma(\theta)$ . As the search space shrinks in one direction, we pass through a crossover region from 2D to 1D. The singular behavior in this intermediate regime can be explained in terms of a recurrent feature observed in our simulations (see also [29]). In this case the walker moves in average towards a given direction, say to the right, in a narrow strip-like space. However, sometimes it turns to an anti-parallel path to visit sites left behind. After some time, the walker ends up in a region depleted of targets, which may be far away from the rightmost point reached by the trajectory. To return to the region rich in unvisited targets located to the right, the walker then needs to make a long jump, as depicted in Fig. 8. Such mechanism is illustrated in Fig. 9, that shows a space-time graph of a simulated

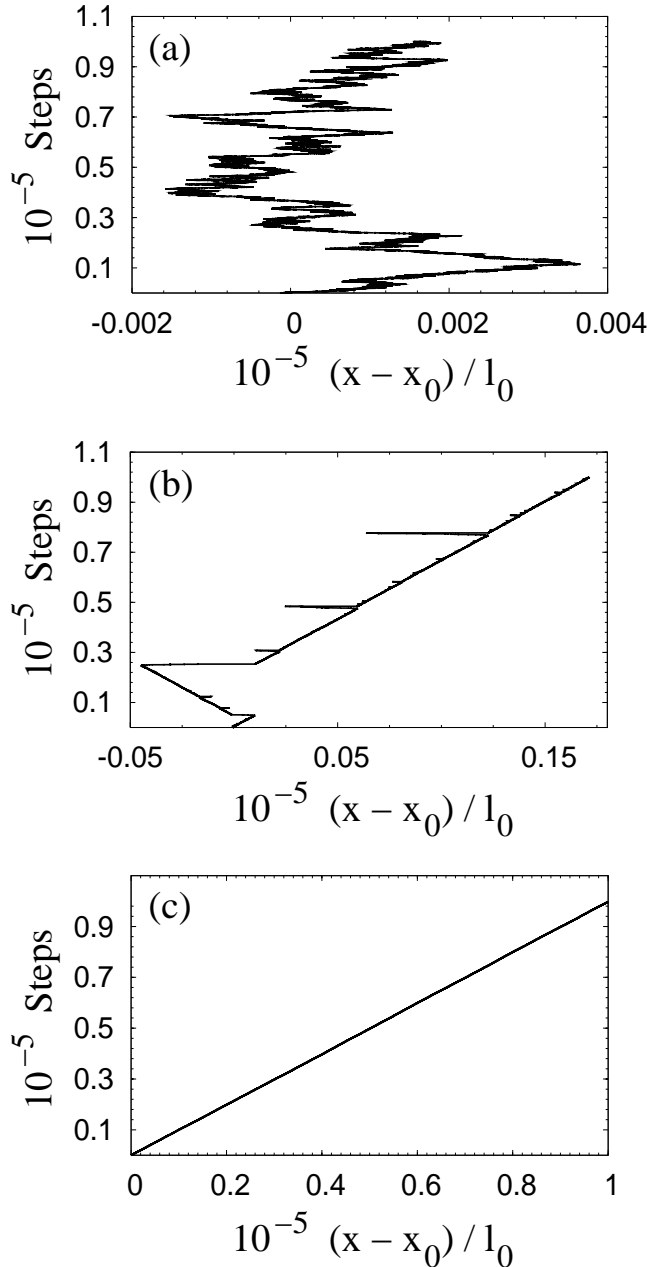


FIG. 9: Number of steps vs. the horizontal projection of the walker position, in the 2D (a), crossover region (b), and 1D (c) cases of Fig. 4. Notice the crucial ultra-long steps at the crossover geometry (b).

trajectory in the three different regimes of Fig. 4.

This dynamical process is particularly sensitive to the distance between the two horizontal borders or equivalently, to the values of  $L/l_0$ . In fact, for very small  $L/l_0$  (1D) there are no anti-parallel paths, whereas for large  $L/l_0$  (2D) the extra vertical direction often provides closer sites than those reached by big jumps across

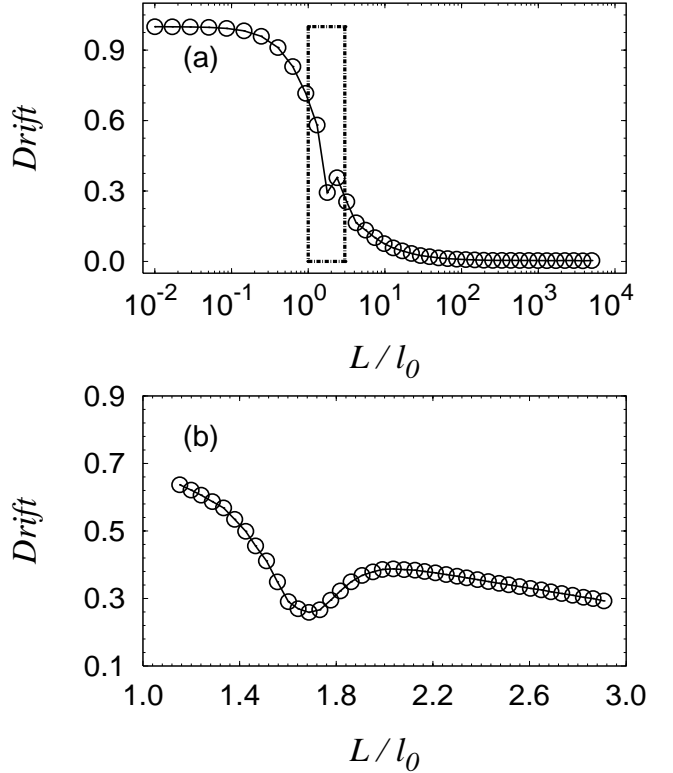


FIG. 10: (a) The numerical drift velocity along  $x$ ,  $\langle |x - x_0|/n \rangle / l_0$ , as a function of  $L/l_0$ . The rectangle indicates part of the crossover region where there is an inflection point for the drift. (b) Blow up of the marked region in (a), showing a local minimum around  $L/l_0 = 1.7094$ . The continuous curves are just guides for the eye.

depleted regions. None of these two aspects, the directional bias in the 1D case and the extra dimension providing many "escape" paths, are present in the crossover region. Note that the broad power-law distributions for the length of the steps  $\ell$  (Fig. 4 (b)) are observed when the probability of large turning angles is high. In the crossover region it is higher than in the 2D regime, as shown in Fig. 7.

The above scenario is confirmed by analyzing two quantities related to the dynamics of the deterministic search process. First, we calculate the normalized drift velocity along the horizontal direction  $x$ , defined as  $\langle |x - x_0|/n \rangle / l_0$ , where  $x_0$  is the starting coordinate and  $x$  is the coordinate at step  $n$ . We show in Fig. 10 (a) the drift velocity as a function of  $L/l_0$ . As expected, it vanishes in the 2D limit. Worthwhile noticing, however, is the behavior of the curve in the crossover region, Fig. 10 (b). In particular, it presents a local minimum around  $L/l_0 = 1.7094$ . Furthermore, the first local maximum after this minimum is at  $L/l_0 = 2.0368 \approx 2$ , the same position for the maximum of  $\ell/l_0$  seen in Fig. 5 (b).

A second relevant quantity is the fraction of visited

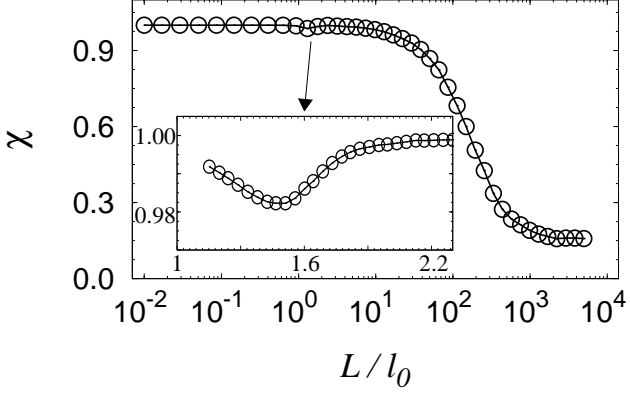


FIG. 11: The numerical fraction of visited targets,  $\chi$ , as a function of  $L/l_0$ . The inset shows a local minimum in the crossover region. The continuous curves are just guides for the eye.

targets along the walker trajectory, defined by

$$\chi = \frac{M_{\text{vis}}}{M_0}. \quad (3)$$

Here,  $M_{\text{vis}}$  is the average number of visited targets in the area searched by the forager and  $M_0$  is the total number of initial targets in that area. The searched area is defined by the region  $[x_{\text{max}} - x_{\text{min}}] \times [y_{\text{max}} - y_{\text{min}}]$ , where the “min” and “max” subscripts stand for the minimum and maximum values of the coordinates reached by the walker during a full run. Thus,  $\chi$  represents a search efficiency of the walker. For the 1D regime, all the targets are found along the way, so  $\chi = 1$ . On the other hand, at 2D regime,  $\chi$  takes a constant small value. The crossover from one limit to the other, as a function of  $L/l_0$ , is shown in Fig. 11. Again we observe a local minimum in the crossover region, as seen in the inset of Fig. 11.

## V. FINAL REMARKS AND CONCLUSION

Motivated by the results of a previous study [29], we have investigated in detail a deterministic walk model where the destructive search environment can be changed from a 2D to a 1D geometry by tuning a single control parameter, namely,  $L/l_0$ . The movement of the walker is driven by the “go to closest target” rule. Naively, the model should lead to a Poisson process, since the initial distribution of target sites (which are destroyed once visited) is random. We actually find that in both the 1D and 2D limiting cases, the step lengths distribution have finite variance. However, for some intermediate values of  $L/l_0$ , a non-trivial dynamical process with infinite variance takes place, combining a large number of relatively small steps with rare long steps. It gives rise to a “Lévy-like” step length distribution, in which the probability

of large steps is enhanced by characteristic exponents in the range  $2 < \mu < 3$ , e.g.,  $\mu \approx 2.2$  for the case in Fig. 4 (b). Furthermore, for values of the control parameter in this crossover region, we observe changes in the search efficiency and drift velocity. Such findings are interesting since they show that power-law distributions can also result from a simple short-range dynamics combined with a geometrical constraint.

Finally, we comment on interesting similarities between our model and other related problems. First, a random foraging model based on Lévy strategies for target sites with a recovery (or regeneration or refractory) delay time [18, 19] has been recently studied. Once visited, a target site become available for a future visit only after a finite number of steps (time delay  $\tau$ ). It has, as limiting regimes, the destructive ( $\tau \rightarrow \infty$ ) and non-destructive ( $\tau \rightarrow 0$ ) random searches. Differently from the present case, the walker may either finish a given step with no target found or truncate its flight if a site is found along its way. In this foraging problem the most efficient destructive (non-destructive) searches requires  $\mu \approx 1$  ( $\mu \approx 2$ ). So, the parameter  $\tau$  makes the crossover from one to other limit. Thus, it seems that the presence of boundaries in the deterministic walk and the time delay in the foraging random search problem play similar roles in the sense that they determine the characteristic exponent for the distribution of the step lengths of the respective walkers, governing then the type of dynamics.

Second, the foregoing results also suggest an analogy between our deterministic walker model and thermodynamic systems and phase transitions. The observed motion in the 2D limit is relatively isotropic, (of course with some bias due to “a back step” depletion), whereas the motion in 1D breaks completely this isotropy. Similarly, the behavior of the velocity is ergodic in the 2-D limit but non-ergodic in 1D limit. Let us now consider more carefully the crossover. Exactly at the point in between the two behaviors, we expect the velocity to be marginally ergodic, such that the average behavior of the velocity inversion becomes log-periodic rather than periodic (2D limit) or nonperiodic (1D limit). Log-periodic velocity inversions [30] can represent the border between superdiffusive and diffusive regimes. Moreover, this logarithmic behavior implies that mean values of  $\ell(t)/l_0$  will scale geometrically with time  $t$ , such that the mean value of  $\ell$  diverges. In other words, the larger the system size (or simulation time), the larger the mean value of  $\ell$ . Except for the memory or correlation effects, this is the same kind of behavior we find in Lévy walks. The maximum superdiffusion for Lévy walks occurs when the first moment of the mean step size diverges, which corresponds to an inverse square distribution of  $\ell$ . Considered from this point of view, the results in Figs. 4 (b) and 5 make qualitative sense.

Thus, although the present study indicates that the system is going through a crossover between two different limits, from the above discussion we cannot completely rule out the possibility of a dynamical phase transition.

This issue is presently being investigated and will be reported in the due course.

### Acknowledgments

Luz, Raposo, Santos and Viswanathan acknowledge CNPq, CNPq/Editoral Universal, FACEPE, FAPEAL,

Fundaçāo Araucāria and Finep/CT-Infra for research grants and also are greatfull to Prof. Carlos Carvalho for very helpful computational hints. Miramontes and Boyer acknowledge UNAM-DGAPA grant IN118306 and Conacyt grant 40867-F for financial support. Finally, Luz thanks the Physics Institute at UNAM for the kind hospitality during stays in which this work has been developed.

---

[1] R. Metzler and J. Klafter, *Phys. Rep.* **339**, 1 (2000); *ibid. J. Phys. A* **37**, R161 (2004).

[2] G. M. Zaslavsky, *Phys. Rep.* **371**, 461 (2002).

[3] I. Peterson, *The Jungle of Randomness: A Mathematical Safari* (Wiley, New York, 1998).

[4] M. F. Shlesinger, G. M. Zaslavsky, and U. Frisch (Editors), *Lévy Flights and Related Topics in Physics* (Springer, Berlin, 1995).

[5] C. Tsallis, *Phys. World* **10**, 42 (1997).

[6] J. Klafter and I. M. Sokolov, *Phys. World* **18** (8), 29 (2005).

[7] A. I. Saichev and S. G. Utkin, *J. Exp. Theoret. Phys.* **99**, 443 (2004); G. M. Viswanathan, E. P. Raposo, F. Bartumeus, J. Catalan, and M. G. E. da Luz, *Phys. Rev. E* **72**, 01111 (2005).

[8] B. B. Mandelbrot, *The Fractal Geometry of Nature*, (Freeman, New York, 1983).

[9] P. Bak, C. Tand, and K. Wiesenfeld, *Phys. Rev. Lett.* **59**, 381 (1987); *ibid. Phys. Rev. A* **38**, 364 (1988).

[10] M. Paczuski, S. Maslov, and P. Bak, *Phys. Rev. E* **53**, 414 (1996).

[11] M. A. Zaks, *Physica A* **310**, 285 (2002).

[12] B. J. West, P. Grigolini, R. Metzler, and T. F. Nonnenmacher, *Phys. Rev. E* **55**, 99 (1997).

[13] B. Podobnik, P. C. Ivanov, Y. Lee, A. Chessa, and H. E. Stanley, *Europhys. Lett.* **50**, 711 (2000); M. J. Keeling, *Theor. Pop. Biol.* **58**, 21 (2000).

[14] M. Levy and S. Solomon, *Int. J. Mod. Phys. C* **7**, 595 (1996); *ibid.*, 745 (1996); D. Sornette and R. Cont, *J. Phys. I (France)* **7**, 431 (1997).

[15] P. M. de Oliveira, *Theory in Bioscience* **120**, 1 (2001); T. Gisiger, *Biol. Rev.* **76**, 161 (2001); R. E. Ulanowicz, *Biosystems* **64**, 13 (2002);

[16] M. F. Shlesinger and J. Klafter, in *On Growth and Form*, edited by H. E. Stanley and N. Ostrowsky (Nijhoff, Dordrecht, 1986); D. W. Stephens and J. R. Krebs, *Foraging Theory* (Princeton University Press, Princeton, 1987).

[17] G. M. Viswanathan, S. V. Buldyrev, S. Havlin, M. G. E. da Luz, E. P. Raposo, and H. E. Stanley, *Nature* **401**, 911 (1999).

[18] E. P. Raposo, S. V. Buldyrev, M. G. E. da Luz, M. C. Santos, H. E. Stanley, and G. M. Viswanathan, *Phys. Rev. Lett.* **91**, 240601 (2003).

[19] M. C. Santos, E. P. Raposo, G. M. Viswanathan, and M. G. E. da Luz, *Europhys. Lett.* **67**, 734 (2004).

[20] G. Ramos-Fernandez and B. Ayala-Orozco, in *Primates in Fragments: Ecology and Conservation*, edited by L. K. Marsh (Kluwer Academic Press, New York, 2002); G. Ramos-Fernandez, J. L. Mateos, O. Miramontes, G. Cocho, H. Larralde, and B. Ayala-Orozco, *Behav. Ecol. Sociobiol.* **55**, 223 (2004); D. Boyer, G. Ramos-Fernandez, O. Miramontes, J. L. Mateos, G. Cocho, H. Larralde, H. Ramos, and F. Rojas, *Proc. R. Soc. B* **273**, 1743 (2006).

[21] A. M. Reynolds, *Phys. Lett. A* **360**, 224 (2006).

[22] G. Oshanin, H. S. Wio, K. Lindenberg, and S. F. Burlatsky, *J. Phys.: Condens. Matter* **19**, 065142 (2007).

[23] O. Bénichou, C. Loverdo, M. Moreau, and R. Voituriez, *J. Phys.: Condens. Matter* **19**, 065141 (2007).

[24] M. C. Santos, G. M. Viswanathan, E. P. Raposo, and M. G. E. da Luz, *Phys. Rev. E* **72**, 046143 (2005).

[25] C. L. Faustino, L. R. da Silva, M. G. E. da Luz, E. P. Raposo, and G. M. Viswanathan, *Europhys. Lett.* **77**, 30002 (2007).

[26] G. F. Lima, A. S. Martinez, and O. Kinouchi, *Phys. Rev. Lett.* **87**, 010603 (2001); C. A. S. Terçariol and A. S. Martinez, *Phys. Rev. E* **72**, 021103 (2005); S. Risau-Gusman, A. S. Martinez, and O. Kinouchi, *Phys. Rev. E* **68**, 016104 (2003).

[27] H. Freund and P. Grassberger, *Physica A* **190**, 218 (1992); D. Gale, J. Propp, S. Sutherland, and S. Troubetzkoy, *Math. Intelligencer* **17**, 48 (1995); L. A. Bunimovich, *Asterisque* **286**, 231 (2003); D. Boyer and H. Larralde, *Complexity* **10**, 52 (2005).

[28] L. A. Bunimovich, *Physica D* **187**, 20 (2004).

[29] D. Boyer, O. Miramontes, G. Ramos-Fernández, J. L. Mateos, and G. Cocho, *Physica A* **342**, 329 (2004).

[30] J. C. Cressoni, M. A. A. da Silva, and G. M. Viswanathan, *Phys. Rev. Lett.* **98**, 070603 (2007).